

Published in final edited form as:

Microcirculation. 2005 June ; 12(4): 313–326. doi:10.1080/10739680590934736.

Differential Coronary Microvascular Exchange Responses to Adenosine: Roles of Receptor and Microvessel Subtypes

JIANJIE WANG*, STEVAN P. WHITT†, LEONA J. RUBIN‡,§, and VIRGINIA H. HUXLEY*§

*Department of Physiology and Pharmacology, School of Medicine, University of Missouri, Columbia, Missouri, USA

†Department of Internal Medicine, University of Missouri, Columbia, Missouri, USA

‡Department of Veterinary Biomedical Sciences, University of Missouri, Columbia, Missouri, USA

§Dalton Cardiovascular Research Center, University of Missouri, Columbia, Missouri, USA

Abstract

Objective—To assess the role of adenosine receptors in the regulation of coronary microvascular permeability to porcine serum albumin (P_s^{PSA}).

Methods—Solute flux was measured in single perfused arterioles and venules isolated from pig hearts using fluorescent dye-labeled probes by microspectro-fluorometry. Messenger RNA, protein, and cellular distribution of adenosine receptors in arterioles and venules were analyzed by RT-PCR, immunoblot, and immunofluorescence.

Results—Control venule P_s^{PSA} ($10.7 \pm 4.8 \times 10^{-7} \text{ cm s}^{-1}$) was greater than that of arterioles ($6.4 \pm 2.8 \times 10^{-7} \text{ cm} \cdot \text{s}^{-1}$; $p < .05$). Arteriolar P_s^{PSA} decreased ($p < .05$) with adenosine suffusion over the range from 10^{-8} to 10^{-5} M, while venular P_s^{PSA} did not change. The nonselective A_1 and A_2 receptor antagonist, 8-(p-sulphophenyl) theophylline, blocked the adenosine-induced decrease in arteriolar P_s^{PSA} . Messenger RNA for adenosine A_1, A_{2A}, A_{2B} , and A_3 receptors was expressed in arterioles and venules. Protein for A_1, A_{2A} , and A_{2B} , but not A_3 , was detected in both microvessel types and was further demonstrated on vascular endothelial cells.

Conclusion—Arteriolar P_s^{PSA} decreases with adenosine suffusion but not venular P_s^{PSA} . Adenosine A_1, A_{2A} , and A_{2B} receptors are expressed in both arterioles and venules. Selective receptor-linked cellular signaling mechanisms underlying the regulation of permeability remain to be determined.

Keywords

adenosine receptor; arteriole; heart; permeability; swine; venule

In the heart the vasculature is critical for maintaining cardiac function via delivery of O_2 and nutrients, including free fatty acids carried on albumin, to the interstitial spaces around the myocardial cells and transport of metabolic by-products and hormones such as the natriuretic peptides away from the myocytes. Coronary exchange capacity depends on the surface area and permeability of all vessels available for exchange. Adenosine (ADO), a

metabolite of adenine nucleotides, is increased dramatically when an imbalance between oxygen supply and consumption exists under a variety of conditions including hypoxia, ischemia/reperfusion, and inflammation (4,61,62). Subsequently, ADO plays a myriad of important cardioprotective roles, including vasodilatation. Conventionally, it is assumed that permeability properties are either unchanged or affected insignificantly when coronary exchange capacity is assessed under the condition of constant surface area during ADO-induced maximal vasodilatation (37). However, evidence from studies with cultured endothelium (15,54,65), as well as conduit and microvascular vessels (5,12,35) showed that ADO influenced exchange, eliciting predominantly a decrease in permeability. It has been argued that findings from in vivo studies result primarily from a direct response of the endothelium to ADO combined with secondary effects of ADO on exchange mediated by hemodynamics, platelet, neutrophil, and/or mast cell functions.

Recently, we modified the techniques for assessing solute permeability in situ that work best in thin exteriorized tissues devoid of movement, such as mesentery or cheek pouch, to determine the direct influence of ADO on intact coronary microvessels from the thick, beating tissue of the heart (26). Accordingly, arteriolar and venular microvascular trees were isolated from hearts, individual microvessel segments were perfused with micropipettes, and solute flux was measured using fluorescent dye-labeled probes by microspectro-fluorometry. This approach permitted us to separate the direct influence of ADO on intact microvascular barrier properties from secondary ADO-mediated effects on hemodynamics, circulating vascular or peripheral tissue. We found previously that 10^{-5} M ADO reduced permeability to albumin of arterioles (24,26) and venules (25) isolated from hearts of sedentary pigs. Therefore, in the present study, we predicted that ADO would enhance directly the intact microvascular barrier function at doses closer to that found in intact coronary tissue.

Four subtypes of ADO receptors (A_1 , A_{2A} , A_{2B} , and A_3) have been cloned from multiple species, although the data from pigs are incomplete (40,41,61,62). Molecular evidence for ADO A_{2A} receptor expression in cultured endothelium derived from porcine coronary arteries (48) and intact porcine coronary arterioles (21) supports pharmacological data that ADO A_{2A} receptors mediate the dilatation of porcine coronary arteries (21,39). ADO A_{2B} receptor message and protein also have been demonstrated in cultured endothelial cells of porcine coronary arteries (48) and pharmacological evidence exists for A_{2B} receptor involvement in modulation of cell growth (9) and changes in membrane potential (49). Recently, A_1 receptors were found to be expressed in cultured vascular smooth muscle cells and intact porcine coronary conduit arteries (21,46). To date, there are no published data for the existence of A_3 receptors in porcine coronary arteries or arterioles. With respect to the venous side of the coronary vasculature, no literature exists defining the expression of ADO receptors. Therefore, we predicted expression of ADO A_1, A_2 , but not A_3 receptors, in porcine coronary arterioles and venules.

In the present study we tested 2 hypotheses: (1) ADO would decrease permeability in a dose-dependent manner, with no difference between vessel types and (2) ADO A_1 , A_{2A} , and A_{2B} receptors would be expressed in both coronary arteriolar and venular vessels. We characterized the permeability of arterioles and venules isolated from hearts of pigs to PSA under control conditions and in response to cumulative concentrations of ADO (10^{-9} to 10^{-5} M). The nonselective ADO A_1 and A_2 receptor antagonist 8-(p-sulfophenyl)theophylline (8-SPT) was used to elucidate further the role of ADO receptors in the modification of permeability response to ADO. Finally, the expression of mRNA and protein for 4 ADO receptor subtypes in porcine coronary arterioles and venules isolated from the same hearts was determined.

MATERIALS AND METHODS

Experimental Animals

Adult Yucatan miniature swine of both sexes weighing 35–55 kg were procured from a breeder (Charles River, ME). The pigs used in this study were the sedentary counterparts to endurance exercise-trained pigs (28). The sedentary pigs were restricted to their pens except for routine maintenance and feeding for 16–20 weeks prior to experiments. All animal care and research procedures complied with the Guide for the Care and Humane Use of Laboratory Animals issued by the National Institutes of Health under the supervision of the Office of Laboratory Medicine at the University of Missouri.

Heart Preparation

The pigs were sedated with ketamine (25 mg/kg, IM), and rompun (2.25 mg/kg, IM) and anesthetized with sodium pentobarbital (20 mg/kg, IV). Following heparin (1000 U/kg) administration via ear vein, a left thoracotomy was conducted. Hearts were excised and immersed in cold (4°C) mammalian Krebs's solution (38,57).

Preparation of Coronary Arterioles and Venules

For study of coronary microvessel permeability to protein, the right ventricular wall (5–7 by 2–3 cm) was excised, weighed, and pinned into 20-mm-deep culture dishes (Tadcoti, Monrovia, CA) containing Krebs's and 10 mg/mL porcine serum albumin (PSA) at 4°C. Arteriolar and venular plexuses were isolated from surrounding connective and cardiac myocardial tissues as described previously (26,28). Briefly, an arteriolar plexus contained interconnected arterioles that appeared less than 100 μm in internal diameter (ID) and branched from larger feed arterioles (ID > 250 μm) arising originally from the right coronary artery. These interconnected arterioles with ID 5–100 μm could span from the epicardial to endocardial surface and would be defined by Kassab (29) as A₁- to A₆-order vessels. These vessels were mounted gently on a Sylgard pad (Dow Corning, MI) with 0.1-mm Minutten pins at approximately its in situ resting length for the subsequent perfusion and study. In the case of the coronary venules, the plexus generally came from the epicardial surface. The venules, in contrast to the coronary arterioles, were thinner walled, and more irregular in shape. The branching pattern was referred to as fingers collecting into a hand- or mitten-like structure (30). The venular plexus contained venules with ID 30–100 μm , which were defined as V₃- to V₅-order vessels (30).

For determination of messenger RNA and protein for ADO receptors, coronary arterioles and venules following initial isolation were further cleaned, carefully trimming off all fat cells and connective tissue surrounding the vessels. For RT-PCR analysis of mRNA single arterioles (ID < 100 μm , length = 1 mm) or venules (ID < 200 μm , length = 1 mm) were immersed in RNase-free microcentrifuge tubes (Ambion, TX) containing RNA Later (Ambion, TX) to protect RNA from degradation, and then stored at –70°C for subsequent analysis. ADO receptor protein was obtained from 2 isolated arterioles or venules (the same sizes as for RT-PCR) that were pooled and stored at –70°C until immunoblot analysis.

Measurement of Coronary Microvessel Permeability

The details of solute permeability (P_s) measurement in isolated arterioles have been published (26,30,31,59). In this study, a similar approach was used for coronary venules. To summarize, a single microvessel segment in the plexus was cannulated with a beveled glass theta micropipette (WPI, Sarasota, FL) containing an unlabeled washout solution in one half of the theta pipette and labeled test solution with Alexa Fluor 488 (Molecular Probes, OR) in the other half of the pipette. Two pairs of separate manometers controlled perfusion pressures in each half of the pipette.

Fluorescence intensity (I_f) emanating from the perfused microvessel lumen and surrounding microvessel wall was measured on a microscope photometer (PTI, Brunswick, NJ). The detectable fluorescence area was restricted by an adjustable rectangular window at 3 times vessel diameter in width and 2 times vessel diameter in length. Solute flux (J_s) per unit surface area (S) and constant concentration gradient (C), ($J_s/S \Delta C$, $\text{cm}\cdot\text{s}^{-1}$) was determined from the relation:

$$P_s = J_s/S \Delta C = 1/\Delta I_0 (dI_f/dt)_i (D/4) \quad (1)$$

where I_0 is the fluorescence intensity of the test solute filling the microvessel lumen; $(dI_f/dt)_i$ is the initial change in fluorescence intensity as solute moved across the vessel wall, and D is microvessel diameter. To minimize change in diameter and maintain microvessel tone constant, all measurements were performed at 15°C (26,34).

Experimental Protocols

Basal permeability to PSA (P_s^{Control}) of individual isolated coronary microvessels was measured when the vessel was perfused with Krebs's-PSA (10 mg/mL) tagged with Alexa Fluor 488 and superfused with Krebs's-PSA (10 mg/mL) solution, respectively. After acquisition of baseline data, P_s was measured again when the superfusate was changed to ADO solution at serial final concentrations over the range of 10^{-9} to 10^{-5} M. To determine whether ADO receptors mediate the permeability response to ADO, P_s was estimated on the same vessels during suffusion with the nonselective, water-soluble, ADO receptor antagonist, 8-SPT (10^{-4} M), in the absence or presence of ADO after basal permeability measurement. All measurements, repeated a minimum of 3 times under each condition, were carried out at low hydrostatic pressures of 12 cm H₂O in venules and 15 cm H₂O in arterioles, respectively, to minimize contributions of convective coupling or solvent drag to the measure of net flux.

Solutions

The components of the mammalian Krebs's solutions included (in mM): 141.4 NaCl, 4.7 KCl, 2 CaCl₂·H₂O, 1.2 MgSO₄, 1.2 NaH₂PO₄·H₂O, 5 glucose, 3 NaHCO₃, and 1.5 Na-*N*-2-hydroxyethylpiperazine-*N'*-2-ethanesulfonic acid (Hepes). The pH and osmolarity of the solution was 7.40 ± 0.05 and 294 (292–298) mOsm at room temperature.

For stock solutions of Krebs's/porcine serum albumin (>50 mg/mL) of PSA (Sigma, MO) the protein was dissolved in H₂O at a concentration of 100 mg/mL. Diafiltration was performed in an Amicon Stirred Cell (Millipore, MA) through a 30,000 Nominal Molecular Weight Limit (NMWL; Millipore, MA) filter with a volume of glucose-free Krebs's solution equal to 3 times the volume of PSA solution. The concentration of the dialyzed protein was determined by absorbance spectroscopy with 280-nm wavelength, then adjusted to 100 mg/mL stock solution and stored at -70°C. All solutions containing PSA at 10 mg/mL final concentration were prepared and used daily.

PSA labeled with Alexa Fluor 488 (Molecular Probes, OR) fluorescent dye was utilized as molecular probe to detect the properties of coronary microvessel barrier. Alexa Fluor 488 and PSA solution (3:1; molar/ molar) were mixed and reacted for 30 min at room temperature, followed by removal of free fluorescent dye with D-Salt Polyacrylamide Desalting Columns (Pierce, IL). The concentration of protein conjugate was determined with Bradford colorimetric assay (Bio-Rad, CA). The perfusate of fluorescently labeled test solution at 10 mg/mL final concentration of PSA was made up of labeled PSA: unlabeled dialyzed PSA (1:9; weight/weight) in Krebs's solution.

Drugs

ADO (purchased from Sigma Chemical) was prepared from stock solutions on the day of use. A stock solution (10^{-3} M) of ADO was prepared in ddH₂O and diluted to a final concentration (10^{-9} to 10^{-5} M) with Krebs's-PSA (10 mg/mL). 8-SPT was prepared in Krebs's-PSA (10 mg/mL) to final concentration of 10^{-4} M.

RNA Preparation and RT-PCR

RNA from microvessels for RT-PCR was prepared using paramagnetic oligo(dT) polystyrene beads (Dynabeads Oligo (dT)₂₅, Dynal). Single venules (ID < 200 μ m; length = 1 mm) or arterioles (ID < 100 μ m, length = 1 mm) were homogenized in 100 μ L of LiCl lysis buffer. The crude lysate was incubated with magnetic Dynabeads Oligo (dT)₂₅ for 15 min at room temperature. The beads were washed twice with 100 μ L of solution A, and then 3 times with 100 μ L of solution B. The mRNA was eluted from beads by adding 10 μ L RNase-free H₂O. Porcine brain was used as a positive control for ADO receptors (7,53). Total RNA from porcine brain was extracted using the RNeasy Total RNA Isolation System (Promega, CA) according to manufacturer's instruction. Following digestion of DNA to oligonucleotides in the sample with DNase I (Invitrogen), first-strand cDNA synthesis from microvessel mRNA and porcine brain total RNA was conducted using reverse transcriptase Superscript II (Invitrogen, CA) and oligo(dT)₁₂₋₁₈ as the primer of the reaction in a 20- μ L volume by following the manufacturer's instructions. The specific ADO receptor primers for A₁, A_{2A}, A_{2B}, and A₃ are listed in Table 1. Complementary DNA amplification was performed using HotStarTaq DNA polymerase in accordance with the manufacturer's instruction (Qiagen, CA). PCR for ADO A₁, A_{2A}, and A_{2B} receptors was conducted for 45 cycles at 94°C for 45s (denature), 58°C for 1 min (anneal), and 72°C for 1 min (extension) following an initial denaturation step of 95°C for 15 min. A final extension of 72°C for 10 min was added after the 45th amplification cycle. PCR for A₃ receptor was conducted for 39 cycles with the same conditions. PCR products were visualized using 2% (w/v) agarose gel electrophoresis stained with ethidium bromide. To determine the nucleotide sequence of PCR products, bands corresponding to the PCR products were removed from the gel. The cDNA was purified with DNA extraction kit (Qiagen, CA) according to manufacturer's instruction and then was subjected to nucleotide sequencing performed by the DNA core at the University of Missouri in Columbia.

To verify that the PCR product was derived from mRNA for ADO receptors in coronary venules and arterioles, RT-PCR was conducted in the absence of the reverse transcriptase Superscript II as a negative control (negative RT).

Immunoblot Analysis

The expression of ADO receptor protein in porcine coronary venules and arterioles was assessed by immunoblot analysis. Two venules (ID <200 μ m, 1 mm in length) or 2 arterioles (ID <100 μ m, 1 mm in length) per tube were homogenized in solubilization buffer consisting of 50 mM Tris · HCl (pH = 7.4), 6 M urea, and 2% SDS (v/v). Cell lysates were subjected to SDS-PAGE [12% (w/v) for A₁ and A₃; 10% for A_{2A} and A_{2B}], and protein was transferred to polyvinylidene difluoride (PVDF) membrane. The membrane was probed with specific ADO receptor anti-A₁ (1:1000 dilution; Affinity BioReagents, CO), -A_{2A} (1:1000 dilution; Alpha Diagnostic International, TX), -A_{2B} (1:100 dilution; Chemicon, TX), or -A₃ (1:200 dilution; Santa Cruz Biotechnology, TX) antibodies followed by incubation with secondary antibody (horseradish peroxidase conjugated IgG, 1:4000 dilution; Alpha Diagnostic International). Protein was detected by enhanced chemiluminescence (NuGlo; Alpha Diagnostic International).

To confirm antibody specificity for ADO A₁ and A_{2B} receptors, control antigenic peptide (for anti-A₁ and anti-A_{2B} antibodies) competition was performed. Antibodies and antigenic peptides (A₁, antibody: peptide = 1:1, Affinity BioReagents, CO; A_{2B}, antibody: peptide = 1:5, Chemicon, CA) were preincubated overnight at 4°C prior to exposure to the PVDF immunoblotting membrane as described above. To characterize anti-ADO A₃ receptor antibody specificity, PVDF immunoblotting membrane was incubated with rabbit gamma-globulin (1:200 dilution; Jackson ImmunoResearch Laboratories, PA) instead of A₃ receptor antiserum as the primary antibody.

Immunofluorescence

The cellular distribution of ADO receptors A₁, A_{2A}, and A_{2B} in coronary venules and arterioles was determined using dual-color immunofluorescence and confocal laser-scanning microscopy. Cryostat sections (6 μm thick) of isolated coronary venules or myocardium were fixed in methanol: acetone (1:1, -20°C for 10 min). Sections were washed with 0.1 M phosphate-buffered saline (PBS, pH 7.4) and blocked with 5% (v/v) normal goat serum (Jackson ImmunoResearch Laboratories, PA) diluted in PSA for 1 h. Sections were then incubated with dual primary antibodies, anti-ADO receptor A₁ (1:10 dilution), A_{2A} (1:5 dilution), or A_{2B} (1:5 dilution) polyclonal antibodies (used for immunoblot) and anti-eNOS monoclonal antibody (1:5 dilution; BD Transduction Laboratories, CA) at 4°C overnight, followed by 3 washes with PSA. Secondary antibodies used were Alexa Fluor 488-labeled goat anti-rabbit IgG for ADO receptor antibodies (10 μg/mL; Molecular Probes) and Alexa Fluor 568-labeled goat antimouse IgG for eNOS antibody (10 μg/mL; Molecular Probes). Secondary antibodies were applied for 30 min, sections were washed with PSA (×3) and mounted with antifading medium (MOWIOL 4–88, Calbiochem, CA) and viewed with confocal (Radiance 2000 Confocal Microscopy System, Bio-Rad) laser (krypton–argon)-scanning microscopy.

To estimate autofluorescence of cross section of myocardium, sections were performed with omission of the primary and secondary antibody incubations. To determine nonspecific fluorescence of myocardium sections, frozen sections were incubated with only secondary antibodies.

Statistical Analysis

StatView 5.0 software (StatView SE Graphics; Abacus Concepts, Berkeley, CA) was employed for all statistical analysis. Values for p_s^{Control} were skewed positively (the mean of the data exceeded the median), which means that distribution of p_s^{Control} was not normal. p_s^{Control} values are therefore expressed as medians ± median absolute deviations (MAD). Values of the vessel diameters and the permeability response, the ratio of $p_s^{\text{Test}}/p_s^{\text{Control}}$, were normally distributed and are given as the means standard errors of the means (SEM). Mann-Whitney *U* test (6) was used to test for differences in p_s^{Control} between coronary venules and arterioles from sedentary porcine hearts. One sample *t* test was utilized to determine whether p_s^{Test} differed from p_s^{Control} testing the null hypothesis $p_s^{\text{ADO}}/p_s^{\text{Control}}=1$ (47). An asterisk (*) indicates $p < .05$.

RESULTS

Differences in Basal Permeability with Vessel Type

Basal apparent permeability to PSA (p_s^{Control}) of coronary venules ($10.7 \pm 4.8 \times 10^{-7}$ cm s⁻¹, median ± MAD; $n = 15$) was greater than that of coronary arterioles ($6.4 \pm 2.8 \times 10^{-7}$ cm·s⁻¹, median ± MAD; $n = 23$) ($p < .05$). The internal diameter (ID) of these isolated

coronary venules and arterioles under basal perfusion conditions was $61.5 \pm 8.19 \mu\text{m}$ (mean \pm SEM) and $44.0 \pm 3.2 \mu\text{m}$, respectively.

Dose-Response to ADO

The permeability responses are paired measures and therefore were expressed as means \pm SE of ratio of P_s in the presence of ADO (P_s^{ADO}) relative to basal permeability of the same vessel in the absence of ADO (P_s^{Control}). The solid line in Figure 1 indicates the ratio ($P_s^{\text{ADO}}/P_s^{\text{Control}}$) equal to 1, identifying a lack of response relative to basal levels. At all doses of ADO tested above 10^{-9} M, a significant decrease in P_s of arterioles was observed ($n = 12$, $p < .05$; Figure 1). The magnitude of the attenuation of arteriolar P_s was 22, 27, 30, and 31% in the presence of 10^{-8} , 10^{-7} , 10^{-6} , and 10^{-5} M ADO, respectively. In contrast, in isolated coronary venules ($n = 7$, Table 2) in response to ADO P_s tended to increase ($P_s^{\text{ADO}}/P_s^{\text{Control}} > 1$) failing, though, to reach statistical significance. Internal diameters of arterioles were significantly increased ($\Delta\text{ID} = 6.7 \pm 2.2 \mu\text{m}$; $n = 11$, $p < .05$) with the application of serial ADO. ADO suffusion did not induce a significant change in coronary venule diameter ($\Delta\text{ID} = 0.7 \pm 0.3 \mu\text{m}$, $n = 7$).

Influence of 8-SPT on the ADO-Induced Decrease in P_s in Coronary Arterioles

The nonselective ADO receptor antagonist, 8-SPT (10^{-4} M), alone was without effect on arteriolar P_s (0.97 ± 0.16 , $n = 10$; Table 2, Figure 2) or basal arteriolar tone. However, the ADO-induced decrease in P_s of arterioles and increase in ID were blocked by 8-SPT (10^{-4} M) over the entire ADO dose–response range ($n = 5-9$, $p < .05$; Figure 2).

Evidence for Messenger RNA for All Four ADO Receptor Subtypes in Porcine Coronary Venules and Arterioles

The presence of mRNA for all 4 ADO receptor subtypes (A_1 , A_{2A} , A_{2B} , and A_3) was found in both coronary venules and arterioles, as shown in Figure 3. The data are representative of RT-PCR analysis ($n = 6-12$). Negative RT (see *RNA Preparation and RT-PCR* under Methods) with the 4 subtype receptor primers demonstrated no bands in the absence of reverse transcriptase, indicating that PCR products resulted from ADO receptor mRNA (data were not shown). The identity of the PCR products from porcine coronary microvessels was verified by direct nucleotide sequencing and BLAST analysis demonstrated 86, 93, 90, and 89% sequence homology with human ADO A_1 , A_{2A} , A_{2B} , and A_3 receptors, respectively.

Pattern of ADO Receptor Protein Expression in Porcine Coronary Venules and Arterioles

Immunoblot analysis revealed expression of ADO A_1 (36 kDa), A_{2A} (54 kDa), and A_{2B} (55 kDa) receptor protein in arterioles and venules, whereas A_3 receptor protein was not detected (Figure 4). The data are representative of immunoblot analysis ($n = 4-10$). Specificity of ADO A_1 , A_{2B} , and A_3 receptor=antibodies for porcine tissue was evaluated by comparison with rat brain tissue that is known to cross-react with these antibodies (Figure 4). Apparent shift of bands between ADO A_{2A} in vascular tissues compared to brain (rat and pig) was not consistent among experiments. In the presence of specific antigenic peptide (for A_1 and A_{2B}) or gamma-globulin (for A_3), bands corresponding to ADO A_1 , A_{2B} , and A_3 receptor proteins were absent (Figure 4). Immunoblots with anti-ADO A_1 , A_{2B} , and A_3 antibodies from porcine brain exhibited the estimated molecular mass of protein bands similar to that of blots from rat brain tissue for A_1 , A_{2B} , and A_3 proteins, respectively (Figure 4). The bands disappeared in immunoblots with control antigenic peptide competition (A_1 and A_{2B}) or gamma-globulin incubation (A_3 ; Figure 4, right panel). These outcomes indicate that the bands shown in Figure 4 are specific.

Cellular Distribution of ADO A₁, A_{2A}, and A_{2B} Receptors in Porcine Coronary Venules and Arterioles

ADO receptors were labeled with green immunofluorescence (Alexa Fluor 488, Figure 5A). Labeled material was observed throughout the cross-sectioned arteriolar and longitudinal sectioned venular wall suggesting receptors were located on cells of the media. To determine whether ADO receptors were also selectively located on endothelial cells, endothelial nitric oxide synthase (eNOS) was identified using red eNOS immunofluorescence (Alexa Fluor 568, Figure 5B) in addition to green ADO immunofluorescence. The yellow color in overlaid images suggests close proximity, if not colocalization, of ADO receptors (A₁, A_{2A}, and A_{2B}) and eNOS (Figure 5C). These findings indicate that ADO A₁, A_{2A}, and A_{2B} receptors exist in endothelial cells of porcine coronary venules and arterioles, and presumably in vascular smooth muscle cells.

DISCUSSION

The present study demonstrates that ADO suffusion reduces apparent P_s^{Control} of arterioles isolated from hearts of normal sedentary pigs in a cumulative dose-dependent manner. This permeability response to ADO appears to be mediated by ADO A₁ or A₂ receptors, as demonstrated by the ability of the nonselective ADO receptor antagonist, 8-SPT, to block the decrease in P_s . Further, this study is the first to provide direct evidence for the expression (mRNA and protein) of 3 ADO receptor subtypes (ADO A₁, A_{2A}, and A_{2B}) in both porcine coronary venules and arterioles. Of interest, in contrast to the behavior of coronary arterioles, in spite of the presence of ADO receptors on venules isolated from the same hearts, suffusion of ADO appeared to be without influence on P_s .

Basal Permeability of Coronary Arterioles and Venules

In the present study the values of P_s^{Control} , 10.7 ± 4.8 and $6.4 \pm 2.8 \times 10^{-7} \text{ cm}\cdot\text{s}^{-1}$ for venules ($n = 23$) isolated from hearts of sedentary pigs, respectively, are in accordance with our previous results (27,57). Venular P_s^{Control} is higher than that for arterioles, which are also consistent with spatial variation of hydraulic conductivity (L_p) in frog capillaries (66). The observed difference in P_s^{Control} between venules and arterioles confirms the assumption of a gradient in permeability coefficients (L_p and P_s) across the microvascular network with high values for venules and lower values for arterioles. The basis for the difference in barrier permeability between venules and arterioles remains unanswered. It is possible that the heterogeneous constituents of vascular walls and/or characteristics of endothelial cells forming the vascular barrier are major factors determining basal permeability. For instance, resistance components of the arteriolar barrier consist of glycocalyx, endothelial cells and smooth muscle cells; the venules presumably have similar glycocalyx, fewer smooth muscle cells, and the endothelial cells cover a larger area with more frequent openings to the basement membrane (43).

The P_s^{Control} of isolated porcine coronary venules reported by Yuan (68) is 5 times higher than our median value for venular basal P_s . Again the basis for this discrepancy is not known and may reflect differences in methodologies and/or conditions, ranging from difference in pig characteristics (breed: Yucatan vs. Yorkshire; age: adult vs. juvenile; body weight: 35–55 kg vs. 8–12 kg) (70), temperature of the suffusion media during measurement of flux (15 vs. 37°C), to the use of porcine vs. bovine serum albumin (3), to the absence vs. presence of India ink gelatin to facilitate visualization of the microvasculature prior to dissection (the points that contrast between the present study with those of Yuan (68), respectively).

The Effect of ADO on Permeability to PSA

Using the technique of measuring P_s in single-perfused microvessels (arterioles and venules) isolated from secondary influences of blood-borne elements, hemodynamics, or tissue associated factors, we demonstrated previously that 10^{-5} M ADO would reduce the P_s to albumin of coronary arterioles (26,35) and venules (25). In the interstitial fluid in the left ventricular epicardium of anesthetized dogs ADO ranged from 4.7 to 9.9×10^{-7} M (13), levels 10- to 20-fold lower than we used previously. The present study extends our previous work on coronary microvessels from pigs by assessing the influence of ADO at physiological and pathophysiological concentrations (from 10^{-9} M to 10^{-5} M) on the exchange barrier permeability to albumin in venules as well as arterioles. These data demonstrate a dose-dependent decrease in P_s^{Control} with increasing ADO concentration, consistent with our earlier work and findings from EC monolayers derived from porcine aorta (65), human umbilical veins (54), and fetal bovine aorta (15). The sensitivity of the ADO response, however, appears greater in intact microvessels (10^{-8} M) than in cultured EC [human umbilical veins (above 10^{-7} M) (54) or fetal bovine aorta (above 10^{-5} M) (15)].

The reduced basal arteriolar P_s in response to ADO suffusion appears to be mediated by ADO receptors, either A_1 or/and A_2 , as the nonselective ADO A_1 and A_2 receptor antagonist 8-SPT (10^{-4} M) blocked the ADO-induced decrease in P_s^{Control} . 8-SPT has been used to validate a role for ADO receptors in cardiovascular regulation in variety of models and species (33,34,60). Unlike other theophylline derivatives, 8-SPT is not an effective phosphodiesterase inhibitor (14), suggesting that changes in P_s are not likely mediated by an indirect action on cyclic nucleotide pathways independent of receptor action. This evidence is supported by the fact that 8-SPT alone did not alter P_s . Rather 8-SPT was effective only against the decreased P_s response of vessels to ADO.

Differences in sensitivity of EC monolayers compared to intact microvessels may reflect differences in expression patterns of ADO receptors, changes in second messenger signaling due to culture conditions or alterations in adenosine uptake and/or metabolism. Metabolism of ADO and generation of reactive oxygen species (superoxide radicals) by the enzyme xanthine oxidase (72) could impact P_s following ADO suffusion. However, increased reactive oxygen species are associated with loss of barrier function and increased hydraulic conductivity (16), the opposite of what we observed in intact arterioles. In EC monolayers, the ADO transport inhibitor, dipyridamole, did not block or enhance the ADO-induced decrease in P_s , suggesting that transport and metabolism is not involved in regulation of the microvascular exchange barrier by ADO (15). These data, as well as evidence showing similar changes in barrier function with the nonmetabolized, ADO receptor agonist 5'-(*N*-ethylcarboxamido) adenosine (NECA), indicate that responses are mediated via binding of ADO to its receptors (65).

The ability of ADO to elicit changes in vessel tone, especially dilatation of coronary arterioles (20), is well known. Although we measure P_s at 15°C to reduce or eliminate ADO-induced vasodilatation, the ID of coronary arterioles increased significantly with ADO suffusion. Accounting for changes in ID would influence the calculation of P_s (Equation 1). An increase in ID would increase P_s . Therefore, the findings of reduction of arteriolar P_s following ADO suffusion could, in fact, be an underestimate of the change in barrier properties.

The observation that ADO failed to alter venular P_s^{Control} significantly contrasts with that for arterioles and a previous report from our laboratory (25). The mechanisms underlying these differential permeability responses are unclear. Gawlowski and Duran (12) reported ADO-induced and dose-dependent increases in venular permeability of hamster cheek pouch,

although these responses may be due to primary and secondary (such as changes in hemodynamics) ADO effects on permeability. Differences observed in the current study, however, appear unlikely due to differential expression of ADO receptor subtypes, since similar subtypes were detected in both vessel types. Instead, with regard to the venular data, it is possible that the sex of the animal plays a role as the venule data in Huxley and Rumbaut (25) were derived primarily from male animals, while in the current study the venules were from both sexes.

Four ADO receptor subtypes, A₁, A_{2A}, A_{2B}, and A₃, have been identified and cloned from a variety of species (41); the exact amino acid sequences of ADO receptors in pig are not known, with the exception of the partial cDNA sequence for ADO A₃ receptors published in BLAST (45). Thus, detection of ADO receptors in the pig has been complicated. For the present study, we designed primers for A₁, A_{2A}, and A_{2B} based on conserved regions in the DNA sequence among several species.

Message and protein expression of A₁ in porcine coronary arterioles and venules differs from data from Hein and co-workers (21) that demonstrated A₁ receptor expression in coronary conduit arteries (left anterior descending artery), but not arterioles. The difference may reflect the age of pigs, 8–12 weeks (21) vs. 16–20 weeks (this study). There exists evidence from studies of ADO effect on cardiovascular functions (18) for enhancement of A₁ receptor sensitivity and reduction of A₂ receptor sensitivity with age. Consistent with our findings of A₁ receptors in microvessels are data from pharmacological studies in coronary resistance arteries from pig (42), mice (10,19), and guinea pig (56). Specifically, studies from Richard et al. demonstrated that the prevention of reactive oxygen species (xanthine/xanthine oxidase)-induced increase in P_s of human umbilical vein endothelial cells by ADO was A₁-mediated (54).

There is substantial evidence from pharmacological and molecular studies supporting the existence of A_{2A} receptors in coronary microvessels and resistance arteries in several species, including pigs. ADO A_{2A} receptors of porcine coronary arterioles appears to account for significant ADO-induced vasodilatation (21). ADO A_{2B} receptor expression has been demonstrated in cultured EC derived from porcine coronary arteries and functional data supports the presence of A_{2B} receptors in porcine (9), human (33), and rat coronary resistance artery (10,22). Data from A_{2A} receptor knockout mice suggest that A_{2B} receptors are involved in regulation of coronary dilatation and growth of arterial endothelial cells (44,63). While studies with cultured EC monolayers provided evidence for A₂ receptors mediating P_s responses to ADO (12), the distinction between receptor subtypes (A_{2A} vs. A_{2B}) was not made. Our data confirm the presence of both A₂ subtypes in arterioles and venules. Consequently, it is not known whether either or both receptor subtypes contribute to the observed permeability responses.

Very little information exists on the distribution and localization of ADO A₃ receptors in coronary vasculature. The only molecular evidence for expression of ADO A₃ receptor is in rat aortic smooth muscle cells (71). Pharmacological studies using a selective ADO A₃ receptor agonist covalently bound to a large polymer suggested the presence of ADO A₃ receptors in luminal coronary resistance arteries of guinea pig hearts (56). In the peripheral circulation, A₃ receptors have been demonstrated on mast cells in the walls of in situ arterioles of the hamster cheek pouch and cremaster muscle preparations (8, 60).

Altogether, this study is the first to characterize the distribution of all 4 identified ADO receptor subtypes in coronary microvessels. The presence of ADO A₁, A_{2A}, and A_{2B} in coronary arterioles and venules as well as on both endothelium and smooth muscle cells contributes significantly to the complications associated with ascribing physiological

functions, such as P_s to a specific receptor subtype. The absence of detectable protein for ADO A_3 receptor in the presence of mRNA for both microvessel preparations could result if protein levels of A_3 receptor were below the detectable level of the immunoblot assay. Alternatively, the presence of mRNA with lack of protein expression implies the potential capacity to express ADO receptors under as yet unidentified circumstances such as adaptation to exercise training or disease.

Possible Mechanisms Underlying the Modulation of ADO on P_s

The data showed that ADO induced a decrease in arteriolar P_s while having no effect on venular P_s . The difference in P_s responses between these microvessel types was clearly not due to differential expression of receptor subtypes on either endothelium or smooth muscle. Because our data are not quantitative, in that the microvessels yielded insufficient material to determine the amount of mRNA and protein loaded on the gels, it is not possible to conclude whether there are differences in receptor density between the 2 vessel types, one mechanism that could contribute to the differences in P_s responses to ADO observed in arterioles versus venules.

Although several signaling pathways reportedly associate with each of the ADO receptor subtypes, it is well documented that A_{2A} and A_{2B} receptors couple to G_s protein with resulting increases in cyclic AMP (cAMP) levels on activation (11,50,59,65). In contrast, A_1 and A_3 receptors couple to G_i protein and activation results in reduction of cAMP levels (11,23). Increases in cAMP levels are associated with decreased P_s in endothelial monolayer (36) and intact microvessel (2). Conversely, reduction of cAMP levels increased P_s of in situ intact microvessels in the absence of other stimuli (17). Molecular evidence for coexistence of ADO A_1 , A_{2A} , and A_{2B} receptors in coronary arteriolar and venular endothelium opens the possibility that coregulatory interactions may determine the net P_s response to ADO. On the other hand, evidence for the expression of A_1 , A_{2A} , and A_{2B} receptors in endothelium does not preclude the involvement of A_3 receptor activation on mast cells in the modulation of P_s by ADO. Mast cells have been found almost exclusively near small human blood vessels without muscle coats and predominantly in the adventitia close to and parallel with the walls of small rat vessels (arterioles and venules) (55). In hamster cheek pouch ADO-induced arteriolar vasoconstriction was mediated by secondary release of histamine and thromboxane from mast cells by activation of A_3 receptors (60). It is well known that histamine induces transient increases in P_s to protein in rat (67) and pig (69), for example. In the present study A_3 receptor protein expression in arterioles was not observed and in the functional study there was no change in P_s from basal levels during exposure to 8-SPT, the putative A_1 and A_2 receptor antagonist. The antagonist data, while providing pharmacological evidence for no role of A_3 in either venules or arterioles fail to provide further information about the role of A_1 and/or A_2 receptor-mediated decrease in P_s observed in the arterioles or the lack of a response to ADO in the venules.

The intracellular levels of cAMP are regulated by the activities of phosphodiesterases (PDE) 2 and 3, which are responsible for the hydrolysis of cyclic nucleotides and cross-talk between cAMP and cGMP pathways (64). In the simplest interpretation, elevation of amount and/or activity of these PDE would result in a decrease in cAMP levels, a situation associated generally with an increase in intact microvessel permeability to water and solutes (1,2,32,51). In several cultured endothelial models, and in the case of the porcine coronary venules, application of ADO resulted in no significant change in venular P_s despite the presence of ADO receptors, especially A_{2AA} and A_{2AB} , whose activation leads to elevation of cAMP. Since the receptors appear to be present in the venules, we hypothesize that either PDE activity differs in the venules and/or the distribution of the PDE isoforms differs between arterioles and venules. There is evidence that PDE isoforms are not evenly distributed along the vascular tree, as Sadhu and coworkers (58) demonstrated PDE2A in the

endothelium of venules and capillaries, but not arterioles, for example. Whether the same is true in the coronary exchange microvascular bed remains to be determined.

The glycocalyx at the surface of vascular endothelial cells has been found to offer a significant resistance to macromolecular solute flux across the vascular barrier of coronary microvessels (27). Further, ADO has been shown to alter permeation of macromolecules into the glycocalyx, potentially altering the net permeation of the macromolecules, such as albumin across the walls of intact microvessels. Specifically, ADO suffusion decreased the ability of the glycocalyx to exclude 70-kDa FITC-dextran from an endothelial cell surface layer of capillaries of hamster cheek pouch (52). While it was shown that ADO still reduced P_s to albumin in arterioles isolated from pig hearts after enzyme treatment to remove the glycocalyx (27) it remains to be determined whether an ADO-induced decrease in the capacity of glycocalyx to exclude albumin is associated with increase in solute flux in coronary microvessels.

Physiological Significance

ADO levels in the heart increase significantly under pathophysiological conditions such as ischemia–reperfusion and inflammation, where hyperpermeability is frequently observed. Vascular hyperpermeability has been thought of as an early indicator of endothelial dysfunction. The distribution of changes in barrier function under conditions of high ADO implies a protective effect of ADO, since reducing P_s at the high pressure end of the coronary vasculature and not altering venular P_s will limit large molecule egress to the low-pressure side of the network. Therefore, the ability of ADO to induce a decrease in arteriolar P_s to albumin under conditions where ADO concentrations rise implies that ADO plays a role in improving or sustaining cardiovascular performance by limiting or slowing loss of barrier function in disease situations associated with endothelial dysfunction.

Most pharmacological studies suggest that A_{2A} receptor activation contributes predominantly to coronary arteriole vasodilatation. The molecular evidence for the existence of 3 receptor subtypes, A_1 , A_{2A} , and A_{2B} , in coronary microvessels implies that the interaction of distinct ADO receptors or/and cellular signaling pathways following ADO binding to these receptors results in the regulation of vascular functions, including dilatation and permeability.

In summary, data from the present study indicate that ADO at physiological and pathophysiological concentrations modulates P_s of arterioles, but not venules, isolated from the hearts of sedentary pigs. The permeability responses to ADO suffusion are dose dependent and appear to be mediated by ADO A_1 and/or A_2 receptor activation. This study is the first to provide molecular evidence for the distribution of ADO receptor subtypes in porcine coronary arterioles and venules. Coexistence of ADO A_1 , A_{2A} , and A_{2B} receptors in endothelial cells of coronary microvessels suggests that interaction of distinct ADO receptor subtypes contributes to change in solute permeability response to ADO.

Acknowledgments

Supported by NIH grant PO1 HL 52490 and NASA grant NAG 5-12300. The authors would like to thank Donna A. Williams for her permission to include some unpublished permeability data generated during her tenure in the laboratory. We also are grateful for Liping Ji, Susan Bingaman, and Steven W. Sieveking's expert technical assistance.

REFERENCES

1. Adamson RH, Curry FE, Adamson G, Liu B, Jiang Y, Aktories K, Barth H, Daigeler A, Golenhofen N, Ness W, Drenckhahn D. Rho and rho kinase modulation of barrier properties: cultured

- endothelial cells and intact microvessels of rats and mice. *J Physiol.* 2002; 539:295–308. [PubMed: 11850521]
2. Adamson RH, Liu B, Fry GN, Rubin LL, Curry FE. Microvascular permeability and number of tight junctions are modulated by cAMP. *Am J Physiol.* 1998; 274:H1885–H1894. [PubMed: 9841516]
 3. Bingaman S, Huxley VH, Rumbaut RE. Fluorescent dyes modify properties of proteins used in microvascular research. *Microcirculation.* 2003; 10:221–231. [PubMed: 12700589]
 4. Bouma MG, van den Wildenberg FA, Buurman WA. The anti-inflammatory potential of adenosine in ischemia–reperfusion injury: established and putative beneficial actions of a retaliatory metabolite. *Shock.* 1997; 8:313–320. [PubMed: 9361340]
 5. Cohen ES, Law WR, Easington CR, Cruz KQ, Nardulli BA, Balk RA, Parrillo JE, Hollenberg SM. Adenosine deaminase inhibition attenuates microvascular dysfunction and improves survival in sepsis. *Am J Respir Crit Care Med.* 2002; 166:16–20. [PubMed: 12091165]
 6. Daniel, WW. Applied nonparametric statistics. PWS-KENT; Boston: 1990.
 7. Dixon AK, Gubitz AK, Sirinathsinghji DJ, Richardson PJ, Freeman TC. Tissue distribution of adenosine receptor mRNAs in the rat. *Br J Pharmacol.* 1996; 118:1461–1468. [PubMed: 8832073]
 8. Doyle MP, Linden J, Duling BR. Nucleoside-induced arteriolar constriction: a mast cell-dependent response. *Am J Physiol.* 1994; 266:H2042–H2050. [PubMed: 8203602]
 9. Dubey RK, Gillespie DG, Jackson EK. A(2b) adenosine receptors stimulate growth of porcine and rat arterial endothelial cells. *Hypertension.* 2002; 39:530–535. [PubMed: 11882603]
 10. Flood A, Headrick JP. Functional characterization of coronary vascular adenosine receptors in the mouse. *Br J Pharmacol.* 2001; 133:1063–1072. [PubMed: 11487517]
 11. Fredholm BB, Abbracchio MP, Burnstock G, Daly JW, Harden TK, Jacobson KA, Leff P, Williams M. Nomenclature and classification of purinoceptors. *Pharmacol Rev.* 1994; 46:143–156. [PubMed: 7938164]
 12. Gawlowski DM, Duran WN. Dose-related effects of adenosine and bradykinin on microvascular permselectivity to macromolecules in the hamster cheek pouch. *Circ Res.* 1986; 58:348–355. [PubMed: 3087654]
 13. Gidday JM, Kaiser DM, Rubio R, Berne RM. Heterogeneity and sampling volume dependence of epicardial adenosine concentrations [see comments]. *J Mol Cell Cardiol.* 1992; 24:351–364. [PubMed: 1619667]
 14. Gustafsson LE. Adenosine antagonism and related effects of theophylline derivatives in guinea pig ileum longitudinal muscle. *Acta Physiol Scand.* 1984; 122:191–198. [PubMed: 6097096]
 15. Haselton FR, Alexander JS, Mueller SN. Adenosine decreases permeability of in vitro endothelial monolayers. *J Appl Physiol.* 1993; 74:1581–1590. [PubMed: 7685754]
 16. He P, Wang J, Zeng M. Leukocyte adhesion and microvessel permeability. *Am J Physiol.* 2000; 278:H1686–H1694.
 17. He P, Zeng M, Curry FE. Dominant role of camp in regulation of microvessel permeability. *Am J Physiol.* 2000; 278:H1124–H1133.
 18. Headrick JP. Impact of aging on adenosine levels, A1/A2 responses, arrhythmogenesis, and energy metabolism in rat heart. *Am J Physiol.* 1996; 270:H897–H906. [PubMed: 8780184]
 19. Headrick JP, Gauthier NS, Morrison RR, Matherne GP. Chronotropic and vasodilatory responses to adenosine and isoproterenol in mouse heart: effects of adenosine a1 receptor overexpression. *Clin Exp Pharmacol Physiol.* 2000; 27:185–190. [PubMed: 10744345]
 20. Hein TW, Belardinelli L, Kuo L. Adenosine A(2a) receptors mediate coronary microvascular dilation to adenosine: role of nitric oxide and ATP-sensitive potassium channels. *J Pharmacol Exp Ther.* 1999; 291:655–664. [PubMed: 10525085]
 21. Hein TW, Wang W, Zoghi B, Muthuchamy M, Kuo L. Functional and molecular characterization of receptor subtypes mediating coronary microvascular dilation to adenosine. *J Mol Cell Cardiol.* 2001; 33:271–282. [PubMed: 11162132]
 22. Hinschen AK, Rose-Meyer RB, Headrick JP. Adenosine receptor subtypes mediating coronary vasodilation in rat hearts. *J Cardiovasc Pharmacol.* 2003; 41:73–80. [PubMed: 12500024]
 23. Hori M, Kitakaze M. Adenosine, the heart, and coronary circulation. *Hypertension.* 1991; 18:565–574. [PubMed: 1937658]

24. Huxley VH. What do measures of flux tell us about vascular wall biology? *Microcirculation*. 1998; 5:109–116. [PubMed: 9789252]
25. Huxley VH, Rumbaut RE. The microvasculature as a dynamic regulator of volume and solute exchange. *Clin Exp Pharmacol Physiol*. 2000; 27:847–854. [PubMed: 11022981]
26. Huxley VH, Williams DA. Basal and adenosine-mediated protein flux from isolated coronary arterioles. *Am J Physiol*. 1996; 271:H1099–H1108. [PubMed: 8853347]
27. Huxley VH, Williams DA. Role of a glycocalyx on coronary arteriole permeability to proteins: evidence from enzyme treatments. *Am J Physiol*. 2000; 278:H1177–H1185.
28. Huxley VH, Williams DA, Meyer DJ Jr, Laughlin MH. Altered basal and adenosine-mediated protein flux from coronary arterioles isolated from exercise-trained pigs. *Acta Physiol Scand*. 1997; 160:315–325. [PubMed: 9338512]
29. Kassab GS. Morphometry of pig coronary arterial trees. *Am J Physiol*. 1993; 265:H350–H365. [PubMed: 8342652]
30. Kassab GS, Lin DH, Fung YC. Morphometry of pig coronary venous system. *Am J Physiol*. 1994; 267:H2100–H2113. [PubMed: 7810711]
31. Kassab GS, Rider CA, Tang NJ, Fung YC. Morphometry of pig coronary arterial trees. *Am J Physiol*. 1993; 265:H350–H365. [PubMed: 8342652]
32. Kasuga F, Inoue S, Asano T, Kumagai S. Effects of isopropanol on the development of inflammatory reactions in rats. *Food Chem Toxicol*. 1992; 30:631–634. [PubMed: 1521838]
33. Kemp BK, Cocks TM. Adenosine mediates relaxation of human small resistance-like coronary arteries via A2b receptors. *Br J Pharmacol*. 1999; 126:1796–1800. [PubMed: 10372822]
34. King AD, Milavec-Krizman M, Muller-Schweinitzer E. Characterization of the adenosine receptor in porcine coronary arteries. *Br J Pharmacol*. 1990; 100:483–486. [PubMed: 2390673]
35. Kutzsche S, Lyberg T, Bjertnaes LJ. Effects of adenosine on extravascular lung water content in endotoxemic pigs. *Crit Care Med*. 2001; 29:2371–3276. [PubMed: 11801842]
36. Langelier EG, van Hinsbergh VW. Nore-pinephrine and iloprost improve barrier function of human endothelial cell monolayers: role of cAMP. *Am J Physiol*. 1991; 260:C1052–C1059. [PubMed: 1709785]
37. Laughlin MH, Overholser KA, Bhatte MJ. Exercise training increases coronary transport reserve in miniature swine. *J Appl Physiol*. 1989; 67:1140–1149. [PubMed: 2551878]
38. Laughlin MH, Pollock JS, Amann JF, Hollis ML, Woodman CR, Price EM. Training induces nonuniform increases in eNOS content along the coronary arterial tree. *J Appl Physiol*. 2001; 90:501–510. [PubMed: 11160048]
39. Lew MJ, Kao SW. Examination of adenosine receptor-mediated relaxation of the pig coronary artery. *Clin Exp Pharmacol Physiol*. 1999; 26:438–443. [PubMed: 10386235]
40. Liang BT. Adenosine receptors and cardiovascular function. *Trends Cardiovasc Med*. 1992; 2:100–108. [PubMed: 21239268]
41. Linden J. Molecular approach to adenosine receptors: receptor-mediated mechanisms of tissue protection. *Annu Rev Pharmacol Toxicol*. 2001; 41:775–787. [PubMed: 11264476]
42. Merkel LA, Lappe RW, Rivera LM, Cox BF, Perrone MH. Demonstration of vasorelaxant activity with an A1-selective adenosine agonist in porcine coronary artery: involvement of potassium channels. *J Pharmacol Exp Ther*. 1992; 260:437–443. [PubMed: 1310735]
43. Michel CC, Neal CR. Openings through endothelial cells associated with increased microvascular permeability. *Microcirculation*. 1999; 6:45–54. [PubMed: 10100188]
44. Morrison RR, Talukder MA, Ledent C, Mustafa SJ. Cardiac effects of adenosine in A(2a) receptor knockout hearts: uncovering A(2b) receptors. *Am J Physiol*. 2002; 282:H437–H444.
45. Murphy WJ, Eizirik E, Johnson WE, Zhang YP, Ryder OA, O'Brien SJ. Molecular phylogenetics and the origins of placental mammals. *Nature*. 2001; 409:614–618. [PubMed: 11214319]
46. Nayeem MA, Mustafa SJ. Protein kinase c isoforms and A1 adenosine receptors in porcine coronary smooth muscle cells. *Vasc Pharmacol*. 2002; 39:47–54.
47. Neter, J.; Wasserman, W.; Kutner, MH. *Applied linear statistical models*. 3rd ed. Richard D. Irwin; Homewood, IL: 1990.

48. Olanrewaju HA. Adenosine A(2a) and A(2b) receptors in cultured human and porcine coronary artery endothelial cells. *Am J Physiol.* 2000; 279:H650–H656.
49. Olanrewaju HA, Gafurov BS, Lieberman EM. Involvement of K⁺ channels in adenosine A2a and A2b receptor-mediated hyperpolarization of porcine coronary artery endothelial cells. *J Cardiovasc Pharmacol.* 2002; 40:43–49. [PubMed: 12072576]
50. Olanrewaju HA, Qin W, Feoktistov I, Scemama JL, Mustafa SJ. Adenosine A(2a) and A(2b) receptors in cultured human and porcine coronary artery endothelial cells. *Am J Physiol.* 2000; 279:H650–H656.
51. Pilati CF, Maron MB. Effect of pathological blood histamine levels on canine coronary vascular permeability. *Am J Physiol.* 1988; 254:H912–H918. [PubMed: 3364595]
52. Platts SH, Duling BR. Adenosine A3 receptor activation modulates the capillary endothelial glycocalyx. *Circ Res.* 2004; 94:77–82. [PubMed: 14630725]
53. Ralevic V, Burnstock G. Receptors for purines and pyrimidines. *Pharmacol Rev.* 1998; 50:413–492. [PubMed: 9755289]
54. Richard LF, Dahms TE, Webster RO. Adenosine prevents permeability increase in oxidant-injured endothelial monolayers. *Am J Physiol.* 1998; 274:H35–H42. [PubMed: 9458849]
55. Riley JF. The relationship of the tissue mast cells to the blood vessels in the rat. *J Pathol Bacteriol.* 1953; 65:461–469. [PubMed: 13062046]
56. Rubio R, Ceballos G. Sole activation of three luminal adenosine receptor subtypes in different parts of coronary vasculature. *Am J Physiol.* 2003; 284:H204–H214.
57. Rumbaut RE, Huxley VH. Similar permeability responses to nitric oxide synthase inhibitors of venules from three animal species. *Microvasc Res.* 2002; 64:21–31. [PubMed: 12074627]
58. Sadhu K, Hensley K, Florio VA, Wolda SL. Differential expression of the cyclic GMP-stimulated phosphodiesterase PDE2a in human venous and capillary endothelial cells. *J Histochem Cytochem.* 1999; 47:895–906. [PubMed: 10375378]
59. Schiele JO, Schwabe U. Characterization of the adenosine receptor in microvascular coronary endothelial cells. *Eur J Pharmacol.* 1994; 269:51–58. [PubMed: 7828658]
60. Shepherd RK, Linden J, Duling BR. Adenosine-induced vasoconstriction in vivo: role of the mast cell and A3 adenosine receptor. *Circ Res.* 1996; 78:627–634. [PubMed: 8635220]
61. Shryock JC, Belardinelli L. Adenosine and adenosine receptors in the cardiovascular system: biochemistry, physiology, and pharmacology. *Am J Cardiol.* 1997; 79:2–10. [PubMed: 9223356]
62. Tabrizchi R, Bedi S. Pharmacology of adenosine receptors in the vasculature. *Pharmacol Ther.* 2001; 91:133–147. [PubMed: 11728606]
63. Talukder MA, Morrison RR, Ledent C, Mustafa SJ. Endogenous adenosine increases coronary flow by activation of both A2a and A2b receptors in mice. *J Cardiovasc Pharmacol.* 2003; 41:562–570. [PubMed: 12658057]
64. Tasken K, Aandhal EM. Localized effects of cAMP mediated by distinct routes of protein kinase. *Physiol Rev.* 2004; 84:137–167. [PubMed: 14715913]
65. Watanabe H, Kuhne W, Schwartz P, Piper HM. A2-adenosine receptor stimulation increases macromolecule permeability of coronary endothelial cells. *Am J Physiol.* 1992; 262:H1174–H1181. [PubMed: 1314509]
66. Williams DA. Bradykinin-induced elevations of hydraulic conductivity display spatial and temporal variations in frog capillaries. *Am J Physiol.* 1993; 264:H1575–H1581. [PubMed: 8498571]
67. Wu NZ, Baldwin AL. Transient venular permeability increase and endothelial gap formation induced by histamine. *Am J Physiol.* 1992; 262:H1238–H1247. [PubMed: 1566906]
68. Yuan Y. Permeability to albumin in isolated coronary venules. *Am J Physiol.* 1993; 265:H543–H552. [PubMed: 8368358]
69. Yuan Y, Granger HJ, Zawieja DC, DeFily DV, Chilian WM. Histamine increases venular permeability via a phospholipase c-NO synthase-guanylate cyclase cascade. *Am J Physiol.* 1993; 264:H1734–H1739. [PubMed: 7684577]

70. Yuan SY, Ustinova EE, Wu MH, Tinsley JH, Xu W, Korompai FL, Taulman AC. Protein kinase C activation contributes to microvascular barrier dysfunction in the heart at early stages of diabetes. *Circ Res.* 2000; 87:412–417. [PubMed: 10969040]
71. Zhao Z, Francis CE, Ravid K. An A3-subtype adenosine receptor is highly expressed in rat vascular smooth muscle cells: Its role in attenuating adenosine-induced increase in camp. *Microvasc Res.* 1997; 54:243–252. [PubMed: 9441895]
72. Zimmerman BJ, Granger DN. Reperfusion injury. *Surg Clin North Am.* 1992; 72:65–83. [PubMed: 1731390]

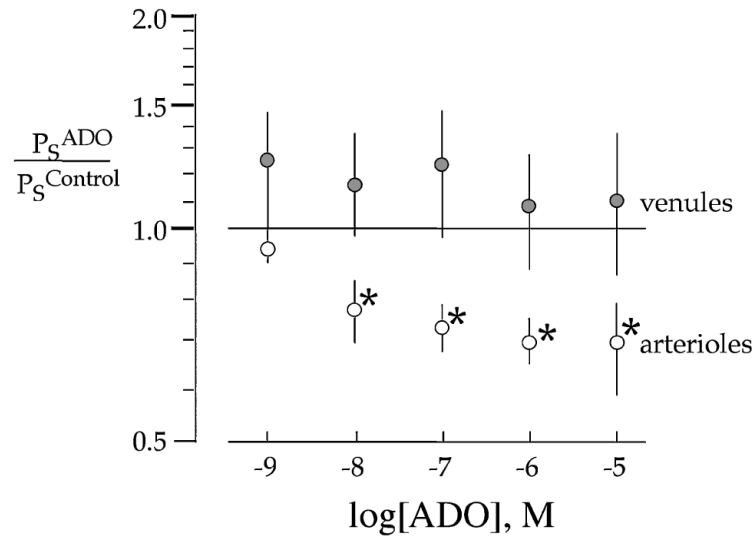


Figure 1.

ADO induces a significant decrease in P_s^{PSA} in arterioles isolated from sedentary pig hearts while being without effect on the P_s of isolated coronary venules. Values are the means \pm SE of ratio of P_s in response to ADO over the range of 10^{-9} to 10^{-5} M ADO relative to basal P_s in the absence of ADO ($n = 7$ for venules, $n = 12$ for arterioles). * $p < .05$ vs. 1.

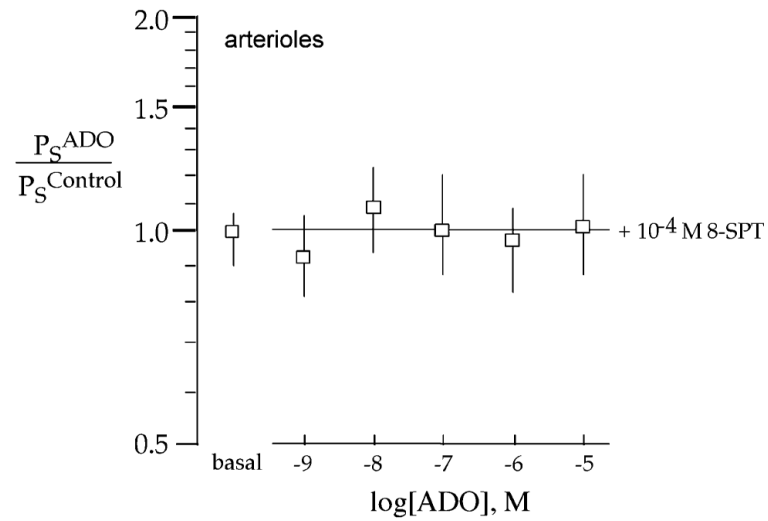


Figure 2.

The nonselective ADO receptor antagonist, 8-SPT (10^{-4} M), blocks the ADO-induced decrease in P_s^{PSA} of porcine coronary arterioles. Means \pm SE of ratio of P_s in response to ADO in the presence of 8-SPT (basal) or ADO is over doses from 10^{-9} to 10^{-5} M relative to the absence of either compound ($n = 5-10$ for ADO in the presence of 10^{-4} M 8-SPT).

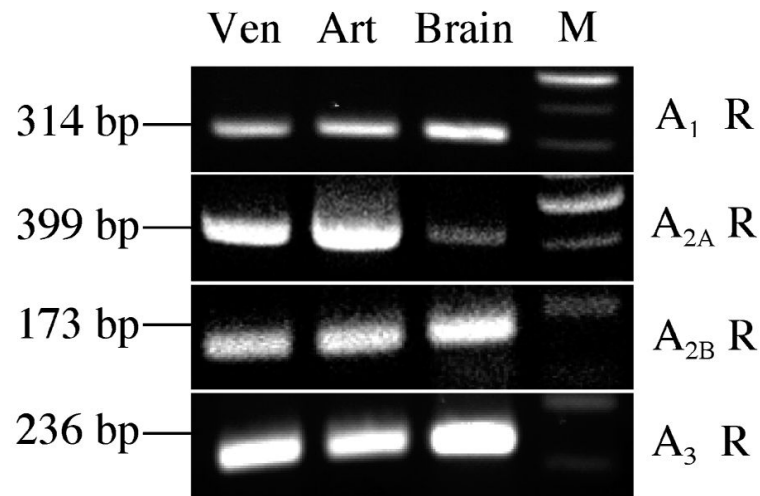


Figure 3.

Messenger RNA for all 4 ADO receptor subtypes (A₁, A_{2A}, A_{2B} and A₃) is expressed in porcine coronary venules and arterioles. RT-PCR analysis with 4 pairs of specific ADO receptor subtype primers was performed on coronary venules and arterioles isolated from the hearts of sedentary Yucatan miniature swine. PCR products were detected with 2% agarose gel stained with ethidium bromide. Representative RT-PCR results are shown ($n = 6-12$). Ven, porcine coronary venules; Art, porcine coronary arterioles; Brain, porcine brain was used as a positive control; M, 100-bp DNA marker ladder.

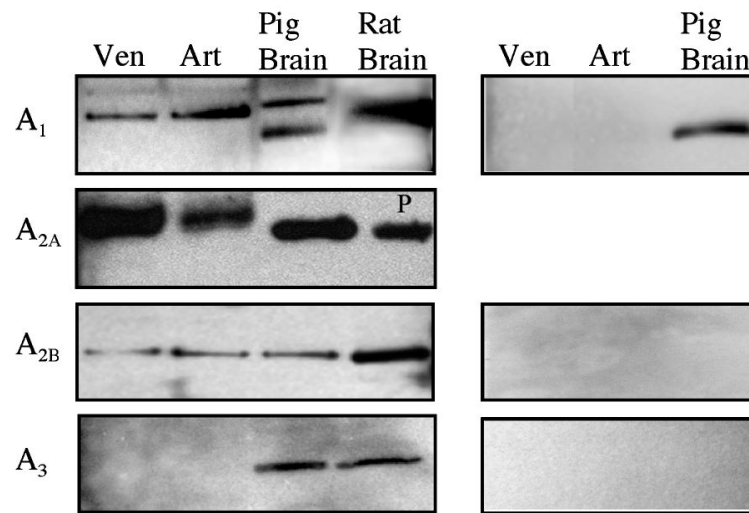


Figure 4. ADO A₁, A_{2A}, and A_{2B}, but not A₃, receptor proteins are expressed in porcine coronary venules and arterioles. Isolated coronary venules (ID < 200 μm) and arterioles (ID < 100 μm) were subjected to immunoblot assay with anti-A₁, -A_{2A}, -A_{2B} and -A₃ antibodies, respectively (left panels). Negative controls are shown in right panels. Representative immunoblots were shown ($n = 4-10$). Ven, coronary venule; Art, coronary arteriole; Brain, pig brain (positive control); and P, positive control (Alpha Diagnostic International, TX).

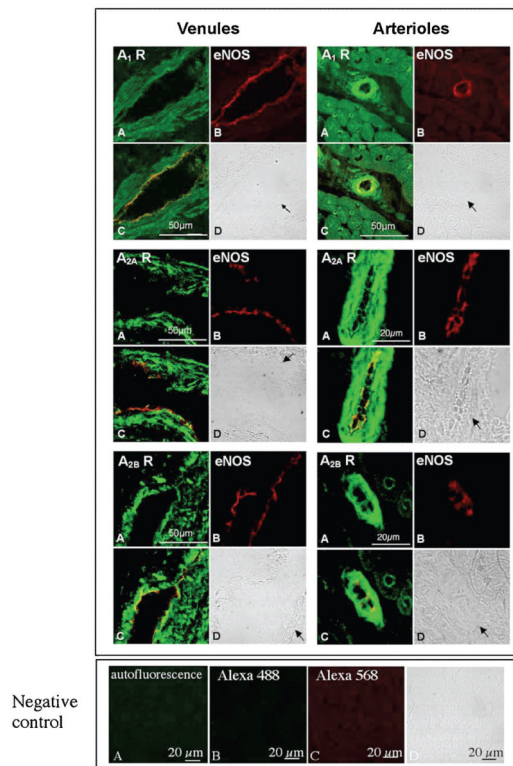


Figure 5.

Immunofluorescent assay demonstrates the presence of ADO A_1 , A_{2A} , and A_{2B} receptor proteins in porcine coronary venules (upper, left panel) and arterioles (upper, right panel), respectively. Coronary preparations were freeze-sectioned for ADO receptor localization in isolated coronary venules and in situ coronary arterioles, respectively. (A) Immunofluorescent staining for ADO receptors with anti- A_1 (top panel), - A_{2A} (middle panel) and - A_{2B} (bottom panel) antibodies, respectively (green); (B) immunofluorescent staining for eNOS (red, as a marker of endothelial cells) with eNOS monoclonal antibody; (C), (A), and (B) overlay that demonstrates expression of ADO A_1 , A_{2A} , and A_{2B} receptors and eNOS in endothelial cells (yellow); and (D) bright field images for coronary venules and arterioles indicated by arrows. In the lower panel, negative controls are shown, including autofluorescence (A), nonspecific staining with omission of primary antibodies (B for Alexa 488, C for Alexa 568), and bright-field image (D).

Table 1

Specific ADO A₁, A_{2A}, A_{2B}, and A₃ receptor primers for RT-PCR

Receptor	Sequence of primer	bp	Size	Accession number
A ₁				
	Forward 5'-GCCACAGACCTACTTCCA-3'	462-479	314	XM_001687
	Reverse 5'-TCCTGGCTGCCTTTATCTA-3'	758-775		
A _{2A}				
	Forward 5'-AACAGCAACTGCAGAACGTCA-3'	380-401	399	XM_000675
	Reverse 5'-TCCTGGCTGCCTTTATCTA-3'	755-778		
A _{2B}				
	Forward 5'-CAAAGTCACTGGGTATGATTGT-3'		173	Olanrewaju et al. (50)
	Reverse 5'-ATAGACAATGGGATTGACAAAC-3'			
A ₃				
	Forward 5'-TTCCGTCATGAGGATGGA-3'	12-19	236	AY 011241
	Reverse 5'-TCCTGGCTGCCTTTATCTA-3'	229-247		

Table 2

The values of ratio ($P_s^{ADO} / P_s^{Control}$) of porcine coronary venular and arteriolar permeability response to ADO

Vessel type	[ADO]						
	Eight-SPT	10 ⁻⁹ M	10 ⁻⁸ M	10 ⁻⁷ M	10 ⁻⁶ M	10 ⁻⁵ M	10 ⁻⁵ M
Venules (n = 7)	1.23 ± 0.24	1.16 ± 0.19	1.21 ± 0.26	1.09 ± 0.19	1.10 ± 0.27	1.10 ± 0.27
Arterioles (n = 12)	0.94 ± 0.12	0.78 ± 0.09*	0.73 ± 0.06*	0.70 ± 0.06*	0.69 ± 0.10*	0.69 ± 0.10*
	0.97 ± 0.16 (n = 10)	0.98 ± 0.11 (n = 9)	0.90 ± 0.13 (n = 8)	1.10 ± 0.18 (n = 7)	0.97 ± 0.15 (n = 6)	0.95 ± 0.15 (n = 5)	0.95 ± 0.15 (n = 5)

Note. Values are expressed as means ± SE. The presence of 10⁻⁴ M 8-SPT.

* p < .05 vs. 1.